

An Analysis of Numerically Simulated Mesovortices and Tornado-like Vortices in a Mesoscale Convective System

Alexander D. Schenkman (alex3238@ou.edu) and Ming Xue (mxue@ou.edu)
School of Meteorology and Center for Analysis and Prediction of Storms
University of Oklahoma, USA

15 September 2009

I. INTRODUCTION

A tornado climatology presented in Trapp et al. (2005) found that up to 20 percent of tornadoes in the United States are spawned by quasi-linear convective systems (QLCS) and bow-echoes. Fujita (1978) presented a conceptual model that summarized the lifecycle of a bow echo from a single ‘tall’ echo to the comma-echo stage during which the bow-echo contains a single cyclonic line-end vortex (hereafter, LEV) at its northern point. Fujita’s conceptual model also proposed that tornadoes and damaging winds were most likely just north of the apex of the bow-echo as well as at the southeastern tip of the comma-echo. More recent studies (e.g., Atkins et al. 2004, Wakimoto et al 2006b, Atkins and St. Laurent 2009a,b) have suggested that tornadoes and damaging winds in these locations of bow echo are spawned by the development of sub-storm scale mesovortices. Mesovortices are typically the parent circulation for the tornadoes spawned by bow-echoes (Trapp and Weisman 2003, Weisman and Trapp 2003, Atkins et al. 2004).

In this study, we use the Advanced Regional Prediction System (ARPS, Xue et al. 2003) model to simulate one such case where several EF-0 and EF-1 tornadoes were spawned by a mesoscale convective system (MCS) that occurred on 8-9 May 2007 in Central Oklahoma. Observations of the MCS show that the tornadoes were associated with mesovortices that developed and rotated around a larger cyclonic LEV. A successful simulation of the both the cyclonic LEV and associated mesovortices was recently obtained by assimilating data from operational WSR-88D Doppler radars and a network of experimental X-band radars of CASA (Center for Collaborative Adaptive Sensing of the Atmosphere) at 2 km and 400 m resolutions (Schenkman et al. (2009a,b), to be submitted to Mon. Wea. Rev.). In the present study, we further refine the grid resolution, by placing a nested 100 m grid within the 400 m grid, starting from the interpolated 400 m initial condition at 0300 UTC. The increased resolution allows us to more closely examine mesovortices as well as the genesis of tornado-like vortices (hereafter, TLVs) in the model.

II. Results

Results from the 100 m simulations show that the model is able to resolve two distinct scales of vortices: mesovortices and smaller scale TLVs. A mesovortex develops in the northern portion of the leading edge of a surging rear-inflow jet around 0315 UTC. The mesovortex has a core-diameter of about 5 km and extends from the surface up to around 2.5 km AGL. TLVs are embedded within the mesovortex circulation. The TLVs are strongest

near the surface and are only present in the lowest kilometer of the atmosphere.

For brevity we present here only fields showing the thermodynamic and kinematic structures of the dominant mesovortex and associated TLVs at 0332 UTC. Figure 1a shows that a strong TLV is present near the surface. The maximum vertical vorticity for this TLV is around 0.4 s^{-1} . The TLV is embedded within a well-defined mesovortex. The mesovortex is most apparent around 1.6 km AGL where the wind field from the TLV no longer obscures the wind field of the mesovortex (Fig. 1b). A current of high θ_e air from east of the mesovortex circulation is wrapping around the mesovortex at this height. Near the surface this high θ_e is present mainly on the south and west sides of the mesovortex. This suggests that a downdraft is likely present to the south and west of the TLV and mesovortex.

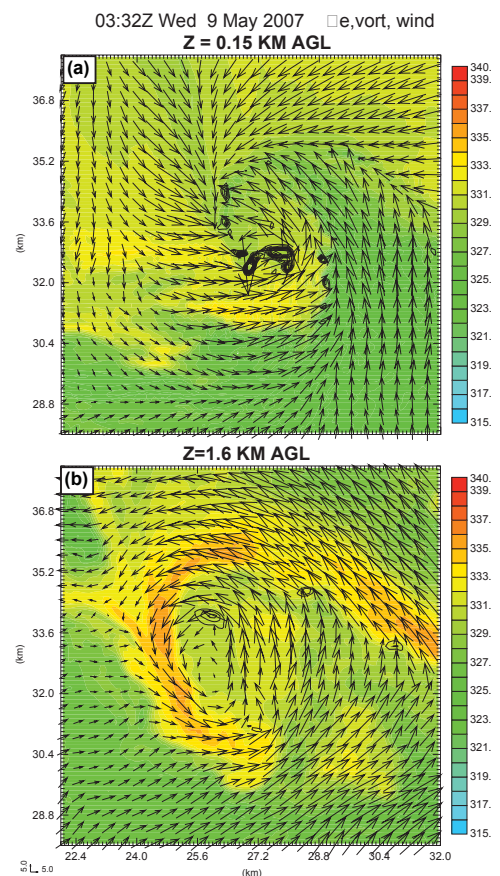


FIG. 1: Horizontal wind vectors, vorticity (contoured in 2×10^{-3} intervals starting at 5×10^{-3}) and θ_e (shaded, K) at 0332 UTC at (a) $Z=150 \text{ m AGL}$ and (b) $Z=1.6 \text{ km AGL}$.

To establish the cause of this downdraft as well as to examine vorticity sources, backward trajectories are calculated for parcels that end up near the surface south of the TLV. These trajectories show that a weak downdraft is present south of the mesovortex (Fig. 2). This downdraft appears to be forced by a downward directed pressure gradient force (PGF) caused by low-level low pressure associated with the TLV.

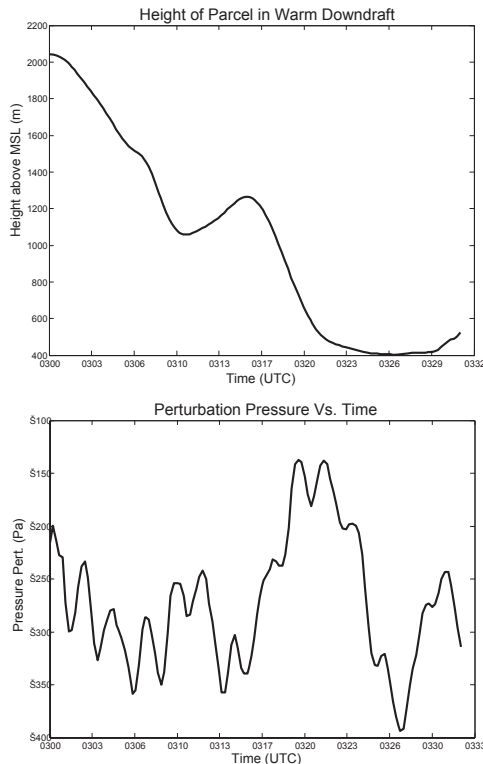


FIG. 1: Time evolution of (top) parcel height and (bottom) perturbation pressure in a weak warm downdraft south of a TLV

A backward trajectory is also calculated for a parcel that terminates within the TLV. Vorticity generation terms via tilting and stretching are calculated for this trajectory (not shown). These calculations show stretching is an order of magnitude larger than tilting suggesting most of the vertical vorticity came from the came from stretching of existing vertical vorticity near the surface.

III. SUMMARY AND CONCLUSIONS

In this extended abstract, results from a 100 m resolution simulation of mesovortices and tornado-like vortices initialized with real data are briefly discussed. These results show that TLVs are embedded within the circulation of a mesovortex. A warm downdraft is generated south of the mesovortex as high θ_e air is forced to descend by a downward directed vertical PGF. Trajectory calculations also show that vorticity is predominantly amplified within TLVs via stretching.

While the preliminary results presented herein have determined the cause of warm downdrafts as well as the dominant vorticity amplification terms, further work is needed to understand the temporal evolution of the mesovortices and TLVs. Additionally, the initial source of vorticity for the TLVs must be determined through more in depth analysis. We seek to obtain a more complete

understanding of the relationship between mesovortices and TLVs.

IV. ACKNOWLEDGMENTS

This work was primarily supported by NSF grant EEC-0313747, as part of ERC CASA. Partial support was also provided by ATM-0530814 and ATM-0802888.

V. REFERENCES

- Atkins N. T., Arnott J. M., Przybylinski, R. W., Wolf R.A., Ketcham K. D., 2004: Vortex Structure and Evolution within Bow Echoes. Part I: Single-Doppler and Damage Analysis of the 29 June 1998 Derecho. *Mon. Wea. Rev.*, 132 2224– 2242
- Atkins N. T., St. Laurent M., 2009: Bow Echo Mesovortices. Part I: Processes that Influence Their Damaging Potential. *Mon. Wea. Rev.*, 137 1497-1513
- Atkins N. T., St. Laurent M., 2009: Bow Echo Mesovortices. Part I: Their Genesis. *Mon. Wea. Rev.*, 137 1514-1532
- Fujita T., 1978: Manual of downburst identification for project Nimrod., 104 pp.
- Schenkman A. D., Xue M. Shapiro A., Brewster K., Gao, J., 2009: Impact of Radar Data Assimilation on The Analysis and Prediction of the 8-9 May Oklahoma Tornadoic Mesoscale Convective System. Part I: Mesoscale Features on a 2 km Grid. *Mon. Wea. Rev.*, To Be Submitted
- Schenkman A. D., Xue M. Shapiro A., Brewster K., Gao J., 2009: Impact of Radar Data Assimilation on The Analysis and Prediction of the 8-9 May Oklahoma Tornadoic Mesoscale Convective System. Part II: Sub-Storm Scale Mesovortices on a 400 m Grid. *Mon. Wea. Rev.*, To Be Submitted
- Trapp R. J., Weisman M. L., 2003: Low-Level Mesovortices within Squall Lines and Bow Echoes. Part II: Their Genesis and Implications. *Mon. Wea. Rev.*, 131 2804-2823
- Trapp R. J., Tessendorf S. A., Godfrey E. S., Brook H. E., 2005: Tornadoes from Squall Lines and Bow Echoes. Part I: Climatological Distribution. *Wea. and forecasting*, 20 23-34
- Wakimoto R. M., Murphey H. V., Davis C. A., Atkins N. T., 2006: High Winds Generated by Bow Echoes. Part II: The Relationship between the Mesovortices and Damaging Straight-Line Winds. *Mon. Wea. Rev.*, 134 2813-2829
- Weisman M. L. Trapp R. J., 2003: Low-Level Mesovortices within Squall Lines and Bow Echoes. Part I: Overview and Dependence on Environmental Shear. *Mon. Wea. Rev.*, 131 2779-2803
- Xue M., Wang D. H., Gao J., Brewster K., Droegemeier K. K., 2003: The Advanced Regional Prediction System (ARPS) Storm-Scale Numerical Weather Prediction Model. *Meteor. Atmos. Physics*, 82 139-170